International Journal of Heat and Mass Transfer 51 (2008) 6102–6109

Contents lists available at ScienceDirect

International Journal of Heat and Mass Transfer

journal homepage: www.elsevier.com/locate/ijhmt

# Modeling of axial bed-to-wall heat transfer in a CFB combustor with abrupt riser exit geometry

Nirmal V. Gnanapragasam [a], B.V. Reddy [b,*]

[a] Department of Mechanical Engineering, University of New Brunswick, Fredericton, NB, Canada E3B 5A3
[b] Faculty of Engineering and Applied Sciences, University of Ontario Institute of Technology, Oshawa, ON, Canada L1H 7K4

ARTICLE INFO

*Article history:*
Received 21 August 2007
Received in revised form 2 May 2008
Available online 21 June 2008

*Keywords:*
Circulating fluidized bed combustor
Axial heat transfer
Riser exit geometry
Heat transfer
Mechanistic and predictive model
Voidage

ABSTRACT

The shape of the riser exit geometry in a circulating fluidized bed (CFB) combustor influences the hydrodynamics of the riser column in the exit region and into the riser column to a considerable length. In the present work, the change in axial hydrodynamics for two different riser exit shapes under different operating conditions is examined to predict the corresponding axial heat transfer coefficients. The influence of the two riser exit shapes (smooth and abrupt) on the axial voidage profile is estimated using the core-annulus mass flux balance model and the corresponding axial bed-to-wall heat transfer coefficient is estimated using the cluster renewal mechanistic model. The results are reported for different hydrodynamic relations and operating parameters. The analysis provides fundamental understanding on the influence of the riser exit geometry on the axial heat transfer characteristics of the CFB combustor.



## 1. Introduction

Circulating fluidized bed (CFB) combustors are popular for power generation using coal and other low grade solid fuels with higher efficiency and reduced pollutants. The exit region of the riser column in CFB combustors allows the passage of suspended solid particles and combustion gases to the cyclone. The flow of entrained solid particles and gases change direction in this zone from vertical to horizontal to exit the riser column and thus changes the hydrodynamics in the exit region as well as the regions below for a considerable length within the riser column. There are two major configurations in the exit design based on the corner shape of the lower part of the exit duct from the riser top: *smooth exit* where the lower part of the exit is smooth with a large radius of curvature and *abrupt exit* where the lower part of the exit is bent with sharp corner and blunt corner (with low radius of curvature) as reported in Harris et al. [1,2].

In commercial CFB risers the radial profiles of the parameters cannot be completely symmetric due to the effects of non-symmetric solids recycling and exit design as reported by Rhodes et al. [3] and Zhou et al. [4]. Effect of exit structure on the axial bed density profile is reported by Brereton and Grace [5] with experimental verification for three different exit geometries. The maximum upward velocity was shifted to the exit side and the wall layer seemed to be thicker on the opposite side as reported by Zhou et al. [6]. Grace [7] observed that the solid particles reach the top of the riser due to their inertia and thereby missing the exit; strikes the top wall and flows back down near the top zone wall of the riser. Pugsley et al. [8] reported that the axial profile of pressure gradient shifted to significantly higher values when the riser was equipped with an abrupt exit and is dependent upon the riser diameter and the particle characteristics. More recent hydrodynamic works based on the exit geometry effects include [9–11,1,2,12,13]. Except the last two, all the others have reported significant experimental data to observe the effect of the riser exit shape on particle concentration in the exit region as well as in the rest of the riser column. Reddy and Nag [14] observed the effect of exit geometry on bed hydrodynamics and heat transfer in a CFB riser column for different operating conditions. Gupta and Reddy [15] proposed a model which uses the exit geometry parameters along with the cluster renewal mechanistic model to estimate and analyze the heat transfer coefficients for changes in the operating and geometry parameters.

There is no investigation (experiments as well as models) available on the axial heat transfer characteristics based on different riser exit geometries. The axial heat transfer process depends on the hydrodynamic parameters and bed temperature. The effect of operating parameters (superficial gas velocity ($U_g$), solids circulation rate ($G_s$) and the local average voidage) on the axial heat transfer with smooth and abrupt exits are not reported. In the current work, the influence of the exit configuration on the axial heat transfer is predicted and analyzed based on the axial mass balance models along with the cluster renewal mechanistic model. The

* Corresponding author. Tel.: +1 905 721 3111x3661; fax: +1 905 721 3370.
*E-mail addresses:* Bale.Reddy@uoit.ca, bv_reddy@hotmail.com (B.V. Reddy).

0017-9310/$ - see front matter © 2008 Elsevier Ltd. All rights reserved.
doi:10.1016/j.ijheatmasstransfer.2008.05.001

**Nomenclature**

| | |
|---|---|
| $c_p$ | specific heat, J/kg K |
| $c_{sf}$ | cluster solid fraction |
| $d_p$ | mean particle size in the bed, μm |
| $e$ | emissivity |
| $f$ | fraction of the wall covered by clusters |
| $g$ | acceleration due to gravity, m/s$^2$ |
| $h$ | bed-to-wall heat transfer coefficient, W/m$^2$ K |
| $h_c$ | cluster heat transfer coefficient, W/m$^2$ K |
| $h_d$ | dispersed (gas) phase convection heat transfer coefficient, W/m$^2$ K |
| $h_r$ | radiation heat transfer coefficient, W/m$^2$ K |
| $k_c$ | thermal conductivity of the cluster, W/m K |
| $Pr$ | Prandtl number |
| $t_c$ | cluster residence time, s |
| $T$ | temperature, K |
| $U_c$ | cluster descent velocity, m/s |
| $U_t$ | terminal velocity of solid particles in the bed, m/s |

*Greek symbols*

| | |
|---|---|
| $\alpha_g$ | thermal diffusivity of the gas, m$^2$/s |
| $\varepsilon$ | volumetric void fraction or voidage |
| $\bar{\varepsilon}$ | cross-sectional average voidage at the considered location |
| $\varepsilon_{an}$ | annulus voidage |
| $\varepsilon_{co}$ | core voidage |
| $\varepsilon_{sm}$ | average voidage in the riser with smooth exit |
| $\varepsilon_{ab}$ | average voidage in the riser with abrupt exit |
| $\delta$ | non-dimensional gas layer thickness between the wall and cluster |
| $\mu_g$ | dynamic viscosity of the gas, N s/m$^2$ |
| $\rho$ | density, kg/m$^3$ |

*Subscripts*

| | |
|---|---|
| b | bed/suspension |
| c | cluster |
| d | dispersed |
| g | gas |
| p | particle |
| w | wall |

work provides the axial heat transfer profile for different operating parameters and riser dimensions. The model begins with the estimation of axial voidage profile using the core-annulus mass flux balance model of He et al. [16] as well as based on the radial voidage correlation of Issangya et al. [17]. Then the corresponding bed-to-wall heat transfer coefficient is estimated using the cluster renewal mechanistic model for each axial location.

## 2. Axial voidage estimation

The voidage in the CFB riser column keeps changing in every cross-section along the height of the riser column. The estimation of axial voidage and the related estimation of axial bed-to-wall heat transfer coefficient is the focus of the current model using two different axial voidage calculation procedures. The first procedure to estimate core-annulus voidage is based on the radial voidage correlation of Issangya et al. [17] and the second procedure is based on the core-annulus mass flux balance model of He et al. [16]. Both the procedures require two steps, one to estimate the annulus thickness along with core and annulus radii and the other to estimate the cross-section averaged voidage based on the thickness of the core and the core-annulus voidage. The estimated cross-section average voidage for each axial location will become the input for the cluster renewal mechanistic model. To account for the riser exit influence, the slip factor is the only input variable to the model that is estimated based on the riser exit shape through the Froude numbers. This makes two different inputs to the model, one for smooth exit (Fig. 1(a)) the other for abrupt exit (Fig. 1(b)). The model formulation starts with the estimation of net cross-section averaged voidage of the suspended bed from the given solids circulation rate as

$$\bar{\varepsilon} = \frac{U_g \rho_p}{G_s \psi - U_g \rho_p} \tag{1}$$

where the slip factor is estimated using the modified relation of Patience et al. [18] by Pugsley and Berutti [19]:

$$\psi = 1 + \frac{5.6}{Fr_g^2} + 0.47 Fr_t^{0.41} \tag{2}$$

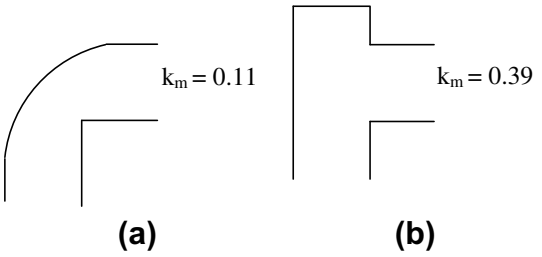


**Fig. 1.** Two different exit configurations used in the analysis: (a) short radius smooth exit and (b) short extension abrupt T exit with respective solids reflux ratios obtained from van der Meer et al. [10].

This correlation is an improved relationship according to Pugsley and Berruti [19] which "better represents the slip factor observed when risers having a diameter exceeding 0.25 m are used, operating at gas superficial velocities lower than 5 m/s". Here, the value of Froude numbers ($Fr_g$ and $Fr_t$) are estimated as given in Harris et al. [1] for the gas velocity and particle terminal velocity. The net particle velocity in the riser column is estimated from the following relation:

$$V_p = \frac{G_s}{\rho_p (1 - \bar{\varepsilon})} \tag{3}$$

The annulus thickness is calculated from the correlation from Harris et al. [20] as given here which varies axial for a given location within the riser column,

$$\delta_a = 0.5D \left[ 0.4014 Re_D^{0.0585} \bar{\varepsilon}^{(-0.0247)} \left( \frac{H - z}{H} \right)^{-0.0663} \right] \tag{4}$$

where $D$ is the hydraulic diameter and thus the thickness of annulus and core on one side of the wall is calculated based on the annulus thickness as simple Cartesian coordinates to prevent over prediction of the core and annulus width:

$$\delta_{an} = 0.5\delta_a \tag{5}$$

$$\delta_{co} = R - \delta_{an} \tag{6}$$

Issangya et al. [17] radial voidage distribution correlation is given as

$$\varepsilon_r = \varepsilon_{mf} + (\bar{\varepsilon} - \varepsilon_{mf})\bar{\varepsilon}^{(-1.5+2.1(r/R)^{3.1}+5(r/R)^{8.8})} \tag{7}$$

The voidage in the annulus is calculated as

$$\varepsilon_{an} = \varepsilon_{mf} + (\bar{\varepsilon} - \varepsilon_{mf})\bar{\varepsilon}^{(-1.5+2.1(\delta_{an}/R)^{3.1}+5(\delta_{an}/R)^{8.8})} \tag{8}$$

The voidage in the core thus becomes

$$\varepsilon_{co} = \frac{\bar{\varepsilon} + \left[\left(\frac{\delta_{co}}{R}\right)^2 - 1\right]\varepsilon_{an}}{\left(\frac{\delta_{co}}{R}\right)^2} \tag{9}$$

The axial voidage distribution estimated using the Issangya et al. [17] does not involve the influence of particle velocities when estimating the core and the annulus voidage which will under predict the axial voidage distribution resulting in inappropriate heat transfer values along the height of the riser. The second procedure to estimate the core-annulus voidage is using the fluid dynamic model proposed by He et al. [16] which gives a better representation of solid particle concentration both in the core and the annulus regions of the CFB riser column. The mass flux balance of core and annulus is obtained on the assumption that in the core zone gas flows upward with some entrained particles with very low particle concentration compared to the wall or the annulus region. In the annulus region particles with higher concentrations and lower velocities flow downwards along the wall. In both core and annulus regions only vertical variation in gas and particle velocities are considered. The difference in the velocities between core and annulus in the horizontal direction are also considered. The mass flux balance of particles in the core region based on core width and voidage is described as

$$\overbrace{u_{pco}\rho_p \frac{d\delta_{co}^2(1-\varepsilon_{co})}{dy}dy}^{\text{net increase of core particle flux}} + \overbrace{2\delta_{co}\rho_p(1-\varepsilon_{co})V_{co\text{-}an}dy}^{\text{transport of particles from core to annulus}} - \underbrace{2\delta_{co}\rho_p[(1-\varepsilon_{an})-(1-\varepsilon_{co})]V_{an\text{-}co}dy}_{\text{transport of particles from annulus to core}} = 0 \tag{10}$$

The mass flux balance of particles in the annulus region based on annulus width and voidage is described as

$$-\overbrace{u_{pan}\rho_p \frac{d\delta_{an}^2(1-\varepsilon_{an})}{dy}dy}^{\text{net increase of annulus particle flux}} - \overbrace{2\delta_{co}\rho_p(1-\varepsilon_{co})V_{co\text{-}an}dy}^{\text{transport of particles from core to annulus}} + \underbrace{2\delta_{co}\rho_p[(1-\varepsilon_{co})-(1-\varepsilon_{an})]V_{an\text{-}co}dy}_{\text{transport of particles from annulus to core}} = 0 \tag{11}$$

As mentioned in the equations the first term represents the net increase of particle flux along the height of the riser column, the second term is related to the transport of particles from the core to the annulus region and last term gives the transport of particles from annulus to the core region. The particle velocity in the core and annulus is estimated using the correlation of Harris et al. [1]:

$$u_{pco} = U_g\left(\frac{R}{\delta_{co}}\right)^2 - U_t \tag{12}$$

$$u_{pan} = U_g\left(\frac{R}{\delta_{an}}\right)^2 - U_t \tag{13}$$

The particle velocity in the annulus $u_{pan}$ is one of the main parameters affecting voidage distribution in the core and annulus. The lateral diffusion velocity of particles from core to the annulus and from annulus to the core respectively are calculated by the correlation of Qi and Farag [21] as given below:

$$V_{an\text{-}co} = 0.0368 + 0.755\left(\frac{gd_p(\varepsilon_{an}-\varepsilon_{mf})}{5(1-\varepsilon_{mf})(1-\varepsilon_{an})}\right)^{0.5} \tag{14}$$

$$V_{eo\ an} = 0.0368 + 0.755\left(\frac{gd_p(\varepsilon_{co}-\varepsilon_{mf})}{5(1-\varepsilon_{mf})(1-\varepsilon_{co})}\right)^{0.5} \tag{15}$$

The radius of the core and annulus are estimated using the Harris et al. [20] correlation and the core and annulus voidage are then estimated by solving Eqs. (10) and (11) using the fourth-order Runge–Kutta method for a system of equations. The voidage estimated for a given axial location depends on the parameters of the previous axial location, so the annulus thickness expression given in Eq. (4) is also estimated one location at a time after updating its cross-section average voidage data for the next step using the expression below:

$$\bar{\varepsilon} = \varepsilon_{an}\left[1 - \left(\frac{\delta_{co}}{R}\right)_{j+1}^2\right] + \varepsilon_{co}\left(\frac{\delta_{co}}{R}\right)_{j+1}^2 \tag{16}$$

Updating the net particle velocity for every average voidage computed along the height is the key in getting the proper axial voidage profile for the respective exit shape of the riser column. The new net cross-section particle velocity is

$$V_p = \frac{G_s}{\rho_p(1-\bar{\varepsilon})} \tag{17}$$

The slip factor for a smooth exit as given by Patience et al. [18] is

$$\psi_{sm} = \frac{U_g}{\bar{\varepsilon}V_p} \tag{18}$$

The average bed voidage per unit length, for a riser with smooth exit is given by Pugsley and Berruti [19] as

$$\varepsilon_{sm} = \frac{U_g\rho_p}{G_s\psi_{sm} + U_g\rho_p} \tag{19}$$

The slip factor for an abrupt exit configuration can be estimated from the relation given below:

$$\psi_{ab} = \psi_{sm}(1+R_f) \tag{20}$$

where $R_f$ is the reflection coefficient defined by Senior and Brereton [22] as the ratio of downward solids in the riser to the upward solids in the riser column which is summarized as

$$R_f = \frac{k_m}{1+k_m} \tag{21}$$

Note that the slip factor for the smooth exit (Eq. (18)) is not dependent on the reflex ratio ($k_m$) of the exit shape, though it is shown in Fig. 1(a), where it represents a small fraction of the solid particles that get reflected back due to the 90° turn at the exit not because of the exit shape. And that $k_m$ value is less significant compared to that of the abrupt exit (Fig. 1(b)). The bed voidage for a riser with abrupt exit is calculated as

$$\varepsilon_{ab} = \frac{U_g\rho_p}{G_s\psi_{ab} + U_g\rho_p} \tag{22}$$

## 3. Axial heat transfer estimation

The hydrodynamic parameters calculated in the predictive model for both the exit shapes are used as input to the cluster renewal mechanistic model [23]. This model is modified with a different correlation for cluster voidage and velocity estimation. The modified cluster renewal mechanistic model will estimate the component and bed-to-wall heat transfer coefficients. The starting parameter for the calculation is the bed average voidage which is the voidage in Eq. (19) for smooth exit and voidage in Eq. (22)

for abrupt exit. The cluster voidage is estimated from the recent correlation given by Harris et al. [24]:

$$\varepsilon_c = 1 - \frac{0.58(1-\bar{\varepsilon})^{1.48}}{0.013 + (1-\bar{\varepsilon})^{1.48}} \tag{23}$$

Here, $\bar{\varepsilon} = \bar{\varepsilon}_{ab}$ or $\bar{\varepsilon} = \bar{\varepsilon}_{sm}$ based on the exit configuration voidage estimated from Eqs. (19) and (22). The shape of cluster, as observed and reported in the CFB literature is mostly used in hydrodynamic models on clusters as primitive geometries such as sphere and cylinder [25,26]. By using a simple force balance between the gravitational force and the buoyant force, the second cluster descent velocity which includes the effects of cluster mass, size and shape is given by

$$U_c = \left(\frac{2m_c g}{C_D \rho_g A_c}\right)^{0.5} \tag{24}$$

The shape is chosen to be a sphere for calculating the mass, area and Reynolds number of the cluster. The mass of the cluster is obtained using the basic definition of mass, $m_c = \rho_c\left(\pi\frac{1}{6}d_c^3\right)$ where the volume of the cluster is the volume of a sphere (the cluster size varies with values of about 1–2 cm being an average size of the cluster as reported in Harris et al. [24] for measured values of cluster sizes from different experimental data). The characteristic travel (descent) length ($L_c$) is the distance descended by the cluster before it disintegrates near the wall in a CFB unit and its value is estimated by the correlation of Wu et al. [27]:

$$L_c = 0.0178\rho_b^{0.596} \tag{25}$$

The suspension density is estimated using the voidage information for the corresponding riser exit shape, i.e., $\bar{\varepsilon} = \bar{\varepsilon}_{ab}$ or $\bar{\varepsilon} = \bar{\varepsilon}_{sm}$ as

$$\rho_b = (1-\bar{\varepsilon})\rho_p + \bar{\varepsilon}\rho_g \tag{26}$$

The component heat transfer coefficients are given below starting with the particle convection heat transfer coefficient is calculated as

$$h_p = \frac{1}{\frac{1}{h_c} + \frac{1}{h_w}} = \frac{1}{\left(\frac{\pi t_c}{4k_c\rho_c c_{pc}}\right)^{0.5} + \frac{d_p\delta}{k_g}} \tag{27}$$

The gas convection heat transfer coefficient to water–wall surfaces is estimated from the Wen and Miller [28] correlation proposed for the dust-laden gas as

$$h_d = \frac{k_g c_p}{d_p c_g}\left(\frac{\rho_d}{\rho_p}\right)^{0.3}\left(\frac{U_t^2}{g d_p}\right)^{0.21} Pr \tag{28}$$

The thermal radiation between the cluster and the wall can be considered as two parallel planes due to the size of the cluster and the radiation heat transfer coefficient is given as [29]

$$h_{rc} = \frac{\sigma(T_b^4 - T_w^4)}{(1/e_c + 1/e_w - 1)(T_b - T_w)} \tag{29}$$

The thermal radiation between the dispersed particle and the wall can again be considered as two parallel planes due to the size of the dispersed phase and the radiation heat transfer coefficient is

$$h_{rd} = \frac{\sigma(T_b^4 - T_w^4)}{(1/e_d + 1/e_w - 1)(T_b - T_w)} \tag{30}$$

Radiation heat transfer coefficient is a combination of radiation from the clusters and from the dilute phase and is given by

$$h_{rad} = f h_{rc} + (1-f)h_{rd} \tag{31}$$

The fractional wall coverage ($f$) by clusters is given by Lints and Glicksman [30] as

$$f = 3.5(1-\bar{\varepsilon})^{0.37} \tag{32}$$

The fractional wall coverage depends on dilute and dense phase operating conditions. The bed-to-wall heat transfer coefficient in the circulating fluidized bed riser is given as the combination of the component heat transfers:

$$h = h_{conv} + h_{rad} = f h_p + (1-f)h_g + f h_{rc} + (1-f)h_{rd} \tag{33}$$

## 4. Assumptions

- The correlations used in the models abide by each of the correlation's specific range and limitations especially riser dimensions and operating conditions.
- The bottom bed has very low voidage giving rise to very steep particle velocity gradients and thus fluctuating heat transfer coefficients so the bottom portion of the bed is not shown in Figs. 4–8 and that is the reason for the curves crossing the ordinate for the maximum heat transfer coefficient (right vertical line).
- The operating conditions and parameters are fixed with respect to time.

## 5. Results and discussion

The results are provided here for both Issangya et al. [17] and He et al. [16] axial voidage distributions along the height. The riser height and diameter are 24.5 m and 4.7 m, respectively, the same dimensions used by He et al. [16]. The range of operating parameters and conditions used in the calculations are listed in Table 1. The radiuses of curvature for smooth and abrupt exits are 0.13 and 0.07, respectively, and the solids reflux ratio for the abrupt exit is 0.39.

### 5.1. Axial voidage profiles

The core and annulus regions within the fully developed flow region of the CFB riser column are one of the most distinctive features of the CFB process which helps in enhanced heat transfer from the gas–solid suspension to the water–walls. The axial voidage distribution in the core and annulus are estimated using the relations in Eqs. (8) and (9) by Issangya et al. [17] and in Eqs. (10) and (11) by He et al. [16]. Fig. 2 shows the axial cross-section averaged voidage for the two riser exit shapes. The Issangya et al. [17] distribution shows better distinction for smooth and abrupt exit shapes but it decreases almost linearly with height

**Table 1**
Values of the operating parameters and physical properties of solid particles and gas used in the analysis

| | |
|---|---|
| Bed temperature, $T_b$ | 1100 K |
| Wall temperature, $T_w$ | 600 K |
| Solids circulation rate, $G_s$ | 30 and 60 kg/ms$^2$ |
| Bed solid particle (sand) size, $d_p$ | 250 μm |
| Superficial gas velocity, $U$ | 4 and 6 m/s |
| Emissivity | $e_p = 0.85$; $e_w = 0.7$; $e_c = 0.5(1 + e_p)$; $e_d = [e_{dp}(e_{dp}+2)]^{0.5} - e_{dp}$, $e_{dp} = \frac{e_p}{(1-e_p)0.5}$ |
| Physical properties of solid particle (sand) | $\rho_p = 2300$ kg/m$^3$; $k_p = 0.27$ W/m K<br>$c_{pp} = 800$ J/kg K – Values from Incropera [36] |
| Physical properties of gas (air) | $\rho_g = 351/T$ kg/m$^3$<br>$k_g = (5.66 \times 10^{-5})T + 1.1 \times 10^{-2}$ W/m K<br>$C_{pg} = (0.99 + 1.22 \times 10^{-4}T)\times 10^3 - (5.68 \times 10^3 T^{-2}) \times 10^3$ J/kg K<br>$\mu_g = 0.42 \times 10^{-6}T^{2/3}$ N s/m$^2$<br>$T = T_{bed}$ K, Correlations as given in Flamant [37] |

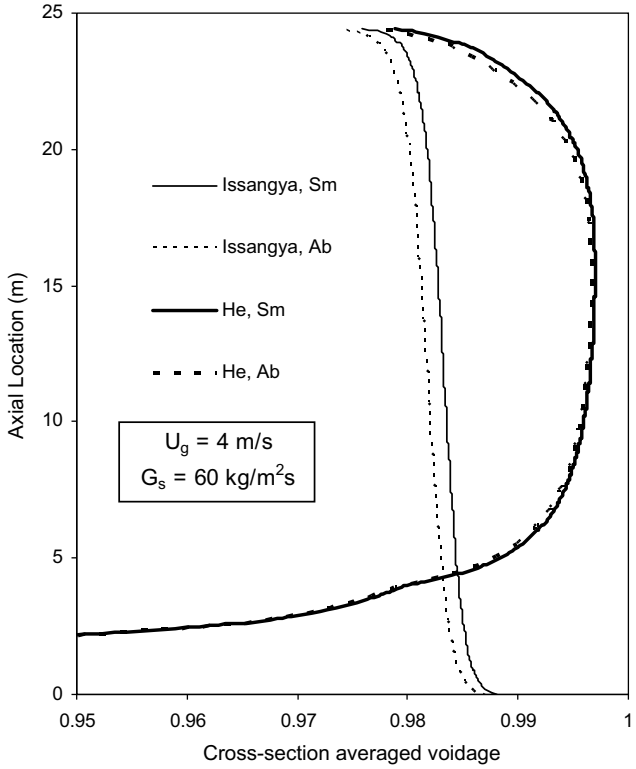


**Fig. 2.** Variation in cross-section averaged voidage along riser height for the two voidage distributions of Issangya et al. [17] and He et al. [16] for the two riser exit shapes.

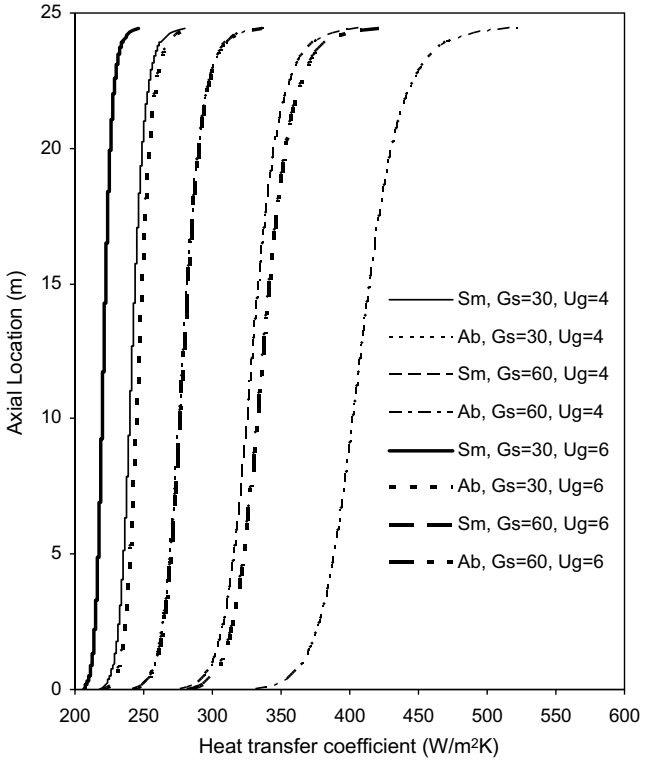


**Fig. 3.** Effect of riser exit shape on axial bed-to-wall heat transfer coefficients for two solids circulation rates (30 and 60 kg/m$^2$ s) and two superficial gas velocities (4 and 6 m/s) based on Issangya et al. [17] for cross-sectional voidage estimation.

forming a reversed S-curve. The lower particle concentration in the bottom is contrary to the accepted voidage profiles [31]. The He et al. [16] axial voidage distribution rather gives a better and another interesting profile of the axial voidage in Fig. 2, though with little difference between the smooth and abrupt exit shapes. The voidage is lower at the bottom (voidage below 95% is not shown in the figure) and gradually increases with height up to one-third of the riser, and remains almost constant before decreasing rapidly in the top region. This is mainly due to the effect of particle velocity estimation based on core and annulus voidage. The He et al. [16] voidage distribution accounts for additional parameters that can provide better axial influence on the voidage estimation. The lateral particle diffusion velocities estimated in Eqs. (13) and (14) account for the particle interaction between the core and the annulus regions. Thus, the voidage predicted is more realistic especially in the top region to account for the exit shapes based on the slip factors calculated for the given radius of curvature.

### 5.2. Effect of superficial gas velocity ($U_g$) and solids circulation rate ($G_s$) on axial bed-to-wall heat transfer coefficient

#### 5.2.1. Axial voidage distribution of Issangya et al. [17]

Based on the voidage profiles, the component heat transfer coefficients as well as the bed-to-wall heat transfer coefficient are estimated using the cluster renewal mechanistic model. For gas velocities of 4 and 6 m/s the axial change in bed-to-wall heat transfer coefficient is shown in Fig. 3 with two different solids circulation rates (30 and 60 kg/m$^2$ s) for the two exit shapes. The riser with abrupt exit and large solids circulation rate has the highest heat transfer value along the riser height due to higher solids concentration in the annulus region (annulus thickness increases with decreasing gas velocity). Due to the form of voidage distribution, the heat transfer value is more at the top than at the bottom of the riser.

For a higher gas velocity ($U_g$ = 6 m/s) the curve for $G_s$ = 60 kg/m$^2$ s in Fig. 3 shows significant reduction in heat transfer values when compared with the data in Fig. 3 for the same solids circulation rate. This is because of the dilution of the bed due to higher gas velocity reducing the particle concentration in the core as well as in the annulus (the annulus thickness is reduced). The heat transfer value for both smooth and abrupt riser shapes at 30 kg/m$^2$ s are low and do not change much with change in gas velocity. The Issangya et al. [17] distribution does not give much variation along the height of the riser due to the limited parameter (just average voidage information) used in estimating the voidage profile (Eq. (8)).

#### 5.2.2. Axial voidage distribution of He et al. [16]

The bed-to-wall heat transfer coefficient values based on the He et al. [16] axial voidage distribution (mass flux balance model) for two different solids circulation rates and riser exit shapes are shown in Fig. 4 for gas velocities of 4 m/s and 6 m/s, respectively. The voidage profile is reflected here on the heat transfer coefficient. Higher heat transfer at the bottom with gradual axial reduction until becoming constant towards the top and then increasing rapidly at the top region of the riser column. The effect of the riser exit shape is prominent at the top region for both the gas velocity cases. The riser with higher solids circulation rate at low velocity will have higher heat transfer coefficient at the top owing to the increase in the particle reflux due to the right angle turn of the flow stream as well as the proximity to the riser roof. There is not as much increase in heat transfer in Fig. 4 at the top for the higher gas velocity case (6 m/s) compared with lower gas velocity (4 m/s). Again this is due to the dilution of the bed thereby reducing the particle concentration especially at the top with fewer particles

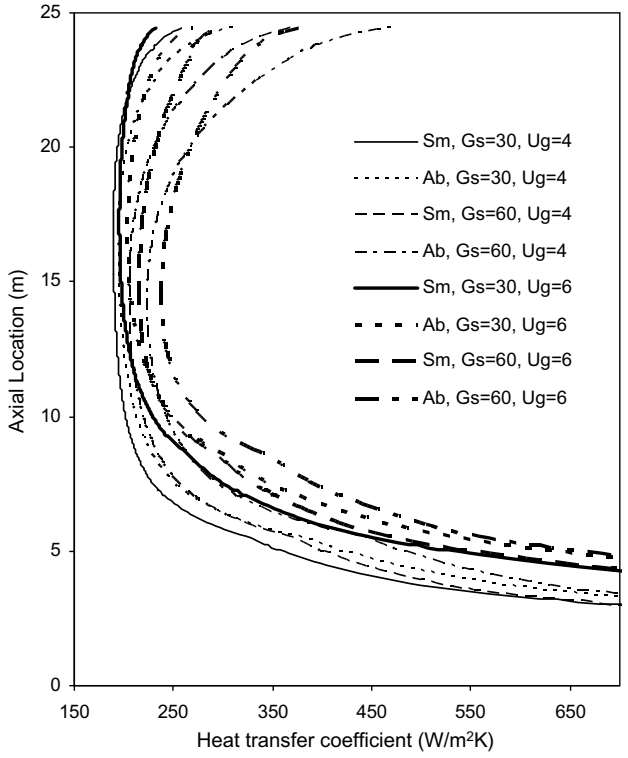


**Fig. 4.** Effect of riser exit shape on axial bed-to-wall heat transfer coefficients for two solids circulation rates (30 and 60 kg/m$^2$ s) and two superficial gas velocities (4 and 6 m/s) based on He et al. [16] for cross-sectional voidage estimation.

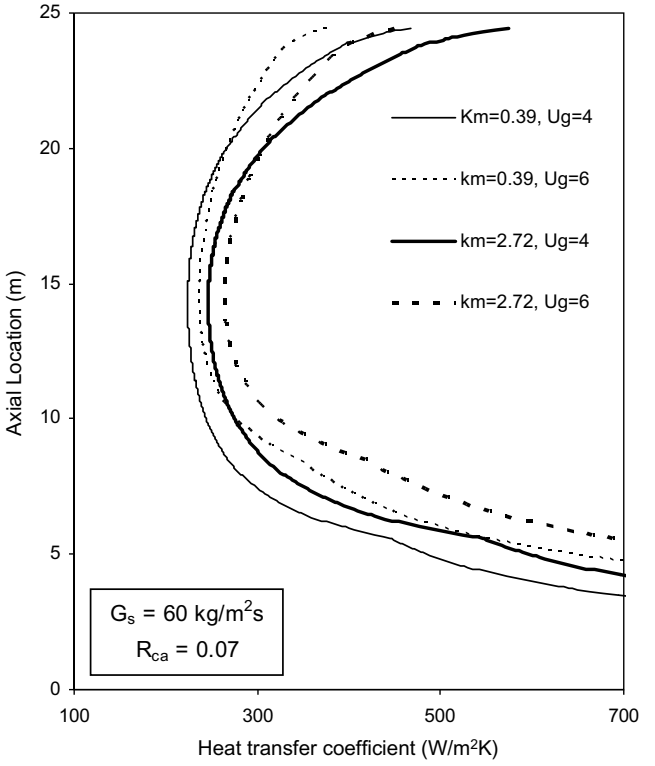


**Fig. 5.** Variation in bed-to-wall heat transfer coefficients along riser height for two different solids reflux ratios and gas velocities for an abrupt exit shape with a radius of curvature of 0.07.

refluxing from the roof of the riser column and more particles carried away along with the gas stream.

### 5.3. Effect of solids reflux ratio and radius of curvature on axial bed-to-wall heat transfer coefficient

The results from Figs. 5–8 are all based on the He et al. [16] axial voidage distribution. The primary parameters that account for the riser exit shape are the solids reflux ratio and radius of curvature. The solids reflux ratio by definition is the ratio of solids downflow in the riser at the entry to the exit and external-solids circulation rate. This parameter accounts for the amount of particles that fall back after hitting the roof of the riser. It is specified as a constant number based on the exit shape. Two different solids reflux ratios (for two abrupt exit shapes) are used for analysis as shown in Fig. 5. The curves for $k_m = 0.39$ represents the short extension blind/abrupt T exit shape and the curves for $k_m = 2.72$ represents the bend/right angle exit shape [10]. The influence on the axial distribution of heat transfer is prominent because of the gas velocity. Within the same gas velocity for the two different solids reflux ratio, heat transfer coefficient increases with increase in the value of $k_m$. This suggests that the higher number of particles reflecting back into the furnace increases the particle concentration at the top as well as down into the riser column thus increasing the heat transfer coefficient.

Fig. 6 shows the bed-to-wall heat transfer value for three different smooth exit shapes based on their radii of curvature. The first one is $R_{cu} = 0.07$ representing the short radius bend exit, the second is with $R_{cu} = 0.13$ representing medium radius bend exit and the third with $R_{cu} = 0.35$ represents long radius bend exit. The radius of curvature is constant for all abrupt exits at 0.07 from experimental findings of van der Meer et al. [10] and Harris et al. [1]. Fig. 6 shows that the short radius bend exit has higher heat transfer

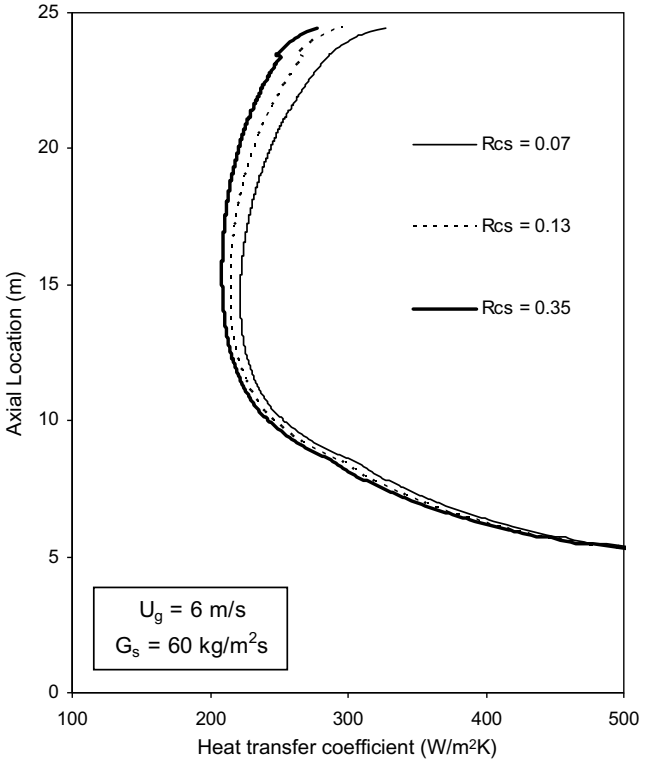


**Fig. 6.** Variation in bed-to-wall heat transfer coefficients along riser height for three different radii of curvatures for a smooth exit shape.

coefficient especially at the top due to its design for higher solids reflux at the top region of the riser column. Along the height the

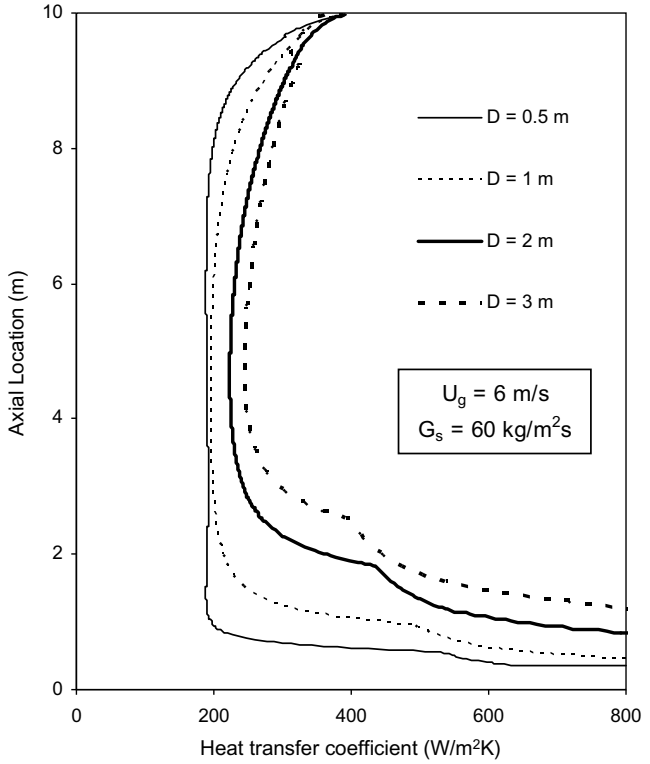


**Fig. 7.** Variation in bed-to-wall heat transfer coefficients along riser height for four different riser diameters for an abrupt exit shape with an height of 10 m.

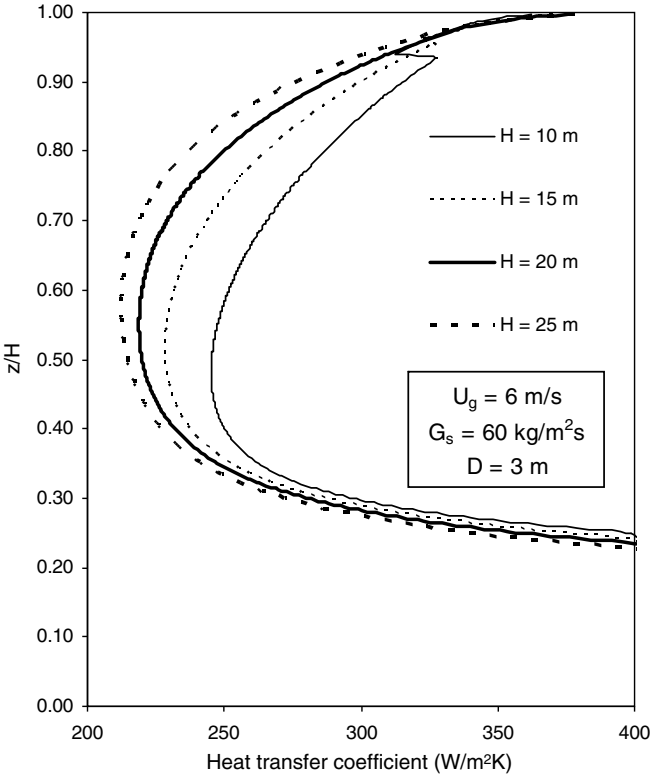


**Fig. 8.** Variation in bed-to-wall heat transfer coefficients along riser height for four different riser heights for an abrupt exit shape with a diameter of 3 m.

heat transfer profile follows the profile of the respective gas velocity and solids circulation rate.

### 5.4. Effect of riser diameter and height on axial bed-to-wall heat transfer coefficient

Knowlton et al. [32] noted that above a riser diameter of roughly 0.15 m, the influence of diameter becomes of lesser importance. The current model predictions are based on annulus and core voidage along the riser height and the correlation in Eq. (4) is used for predicting the annulus thickness which is a function of both riser diameter and height. This correlation was developed from several experimental data including large CFB risers by Harris et al. [20] with an average relative error of 23.9% for the data used to develop the correlation. The range of values of the dimensionless groups involved in Eq. (4) are $1-\bar{\varepsilon}=0.001$—0.3, $(H-z)/H=0.16$–0.87 and $Re=3900$–33,600. Based on this correlation, if there is an increase in diameter, how much will the exit shape affect the heat transfer values is predicted and presented in Fig. 7. It shows the change in bed-to-wall heat transfer coefficient for four different riser diameters having the same height of 10 m. The smaller diameter riser has little variation in heat transfer value along the riser height compared with diameters twice and four times the smaller one. With increase in diameter the heat transfer coefficient increases all along the height. The change in bed-to-wall heat transfer coefficient with different riser heights is shown in Fig. 8 for a fixed riser diameter of 3 m. The heat transfer coefficient decreases with increase in height with higher influence in the middle region of the riser along the height. These two figures give a realistic picture on the influence of riser dimensions on heat transfer coefficient. With lower gas velocity and solids circulation rate, the trends will be reversed like, decrease in heat transfer with increase in the riser diameter or almost no change with change in diameter due to the reduction in solids concentration.

### 5.5. Validation with experimental data and published literature

There are very few experimental data available for axial heat transfer profile without the exit shape information. Ma and Zhu [33] have reported experimental axial heat transfer profiles for riser dimensions and operating conditions different from the current model. The current model results when compared with Ma and Zhu [33] profiles, show similar heat transfer trends and profiles with reasonable agreement (60–70%) under similar range of operating conditions ($G_s$ and $U_g$). The main information conveyed in this work is not in the heat transfer values but in its trends, that is, the riser exit effect on the axial heat transfer behaviour (proportional variation) when there is change in the hydrodynamics due to the changes in operating conditions, exit geometry parameters and riser dimensions. The work also proves the importance of proper core-annulus voidage estimation by comparing two different methods; one by correlation [17] and the other by mass flux balance [16], towards the heat transfer estimation for two riser exit shapes. The difference in the voidage values from the two methods highlights its sensitiveness to global operating conditions thus requiring improved prediction of hydrodynamic parameters especially the core-annulus thickness and voidage. Other works that have reported experimental axial heat transfer profiles in CFB risers without exit effect information include [16,34,35].

## 6. Conclusion

The current work focused on the effect of abrupt riser exit shape on axial bed-to-wall heat transfer coefficient by comparing with smooth riser exit shape. The estimation involved the modeling of axial voidage distribution based on two different predictions and the corresponding heat transfer estimation based on the cluster

renewal mechanistic model. The findings and conclusions from the model and analysis are:

- The effect of solids circulation rate and gas velocity for the two riser exit shapes on the axial heat transfer shows higher heat transfer values for the abrupt exit all along the height with significant difference at the top region.
- Updating the particle velocity for a given solids circulation rate after the axial voidage estimation becomes an important step to appropriately account for the influence of exit shape down the riser column from the top.
- Axial heat transfer coefficient increases with increase in solids reflux ratio and gas velocity for an abrupt exit while not much change is observed for changes in the radius of curvature for a smooth exit.
- For an abrupt exit, the heat transfer increases with increase in the riser diameter with significant difference in the lower portions of the bed rather at the top.
- With increase in height of the riser column, the axial heat transfer decreases significantly for an abrupt exit, especially in the middle portions of the riser column.

## Acknowledgements

The authors kindly acknowledge the financial support for the current project from Natural Sciences and Engineering Research Council of Canada through the Discovery Grant Program. The work was done in the Department of Mechanical Engineering, The University of New Brunswick, Fredericton, NB, Canada.

## References

[1] A.T. Harris, J.F. Davidson, R.B. Thorpe, The influence of exit geometry in circulating fluidized bed risers, AIChE J. 49 (1) (2003) 52–64.
[2] A.T. Harris, J.F. Davidson, R.B. Thorpe, Influence of the riser exit on the particle residence time distribution in a circulating fluidized bed riser, Chem. Eng. Sci. 58 (2003) 3669–3680.
[3] M.J. Rhodes, P. Laussmann, F. Villain, D. Geldart, in: P. Basu, J.F. Large (Eds.), Circulating Fluidized Bed Technology II, Pergamon, New York, 1988, pp. 155–164.
[4] J. Zhou, J.R. Grace, S. Qin, C.M.H. Brereton, C.J. Lim, J. Zhu, Voidage profiles in a circulating fluidized bed of square cross-section, Chem. Eng. Sci. 49 (1994) 3217–3226.
[5] C.M.H. Brereton, J.R. Grace, End effects in circulating fluidized bed hydrodynamics, in: A. Avidan (Ed.), Circulating Fluidized Bed Technology IV, Engineering Foundation, New York, 1994, p. 137.
[6] J. Zhou, J.R. Grace, C.J. Lim, C.M.H. Brereton, Particle velocity profiles in a circulating fluidized bed riser of square cross-section, Chem. Eng. Sci. 50 (1995) 237–244.
[7] J.R. Grace, Influence of riser geometry on particle and fluid dynamics in circulating fluidized bed risers, in: M. Kwauk, J. Li (Eds.), Circulating Fluidized Bed Technology V, Science Press, Beijing, 1996, p. 16.
[8] T. Pugsley, D. Lapointe, B. Hischberg, J. Werther, Exit effects in circulating fluidized bed risers, Can. J. Chem. Eng. 75 (1997) 1001–1010.
[9] S.K. Gupta, F. Berruti, Evaluation of the gas–solid suspension density in CFB risers with exit effects, Powder Technol. 108 (2000) 21–31.
[10] E.H. van der Meer, R.B. Thorpe, J.F. Davidson, Flow patterns in the square cross-section riser of a circulating fluidized bed and the effect of riser exit design, Chem. Eng. Sci. 55 (2000) 4079–4099.
[11] U. Lackermeier, J. Werther, Flow phenomena in the exit zone of a circulating fluidized bed, Chem. Eng. Process. 41 (2002) 771–783.
[12] J. De Wilde, G.B. Marin, G.J. Heynderickx, The effects of abrupt T-outlets in a riser: 3D simulation using the kinetic theory of granular flow, Chem. Eng. Sci. 58 (2003) 877–885.
[13] A. Yan, J.H. Parssinen, J.X. Zhu, Flow properties in the entrance and exit regions of a high-flux circulating fluidized bed, Powder Technol. 131 (2003) 256–263.
[14] B.V. Reddy, P.K. Nag, Effect of riser exit geometry on bed hydrodynamics and heat transfer in a circulating fluidized bed riser column, Int. J. Energy Res. 25 (2001) 1–8.
[15] A.V.S.S.K.S. Gupta, B.V. Reddy, Bed-to-wall heat transfer modeling in the top region of a CFB riser column with abrupt riser exit geometries, Int. J. Heat Mass Transfer 48 (2005) 4307–4315.
[16] Q. He, F. Winter, J.D. Lu, Analysis of the heat transfer mechanism in high-temperature circulating fluidized beds by a numerical model, Trans. ASME 124 (2002) 34–39.
[17] A.S. Issangya, J.R. Grace, D. Bai, J. Zhu, Radial voidage variation in CFB risers, Can. J. Chem. Eng. 79 (2001) 279–286.
[18] G.S. Patience, J. Chaouki, F. Berruti, R. Wong, Scaling considerations for CFB risers, Powder Technol. 72 (1992) 31–37.
[19] T.S. Pugsley, F. Berruti, A predictive hydrodynamic model for circulating fluidized bed risers, Powder Technol. 89 (1996) 57–69.
[20] A.T. Harris, R.B. Thorpe, J.F. Davidson, Characterisation of the annular film thickness in circulating fluidized-bed risers, Chem. Eng. Sci. 57 (2002) 2579–2587.
[21] C. Qi, I.H. Farag, Heat transfer mechanism due to particle convention in circulating fluidized bed, Can. J. Chem. Eng. 72 (1994) 354–357.
[22] R.C. Senior, C. Brereton, Modeling of circulating fluidized-bed solids flow and distribution, Chem. Eng. Sci. 47 (1992) 281–296.
[23] G.N. Vijay, B.V. Reddy, Effect of dilute and dense phase operating conditions on bed-to-wall heat transfer mechanism in a circulating fluidized bed combustor, Int. J. Heat Mass Transfer 48 (2005) 3276–3283.
[24] A.T. Harris, J.F. Davidson, R.B. Thorpe, The prediction of cluster properties in the near wall region of a vertical riser (200157), Powder Technol. 127 (2002) 128–143.
[25] P.D. Noymer, L.R. Glicksman, Cluster motion and particle-convective heat transfer at the wall of a circulating fluidized bed, Int. J. Heat Mass Transfer 41 (1998) 147–158.
[26] P.D. Noymer, L.R. Glicksman, Descent velocities of particle clusters at the wall of a circulating fluidized bed, Chem. Eng. Sci. 55 (2000) 5283–5289.
[27] R.L. Wu, J.R. Grace, C.J. Lim, A model for heat transfer in circulating fluidized beds, Chem. Eng. Sci. 45 (1990) 3389–3398.
[28] C.Y. Wen, E.N. Miller, Heat transfer in solid–gas transport lines, Ind. Eng. Chem. 53 (1961) 51–53.
[29] P. Basu, Heat transfer in fast fluidized bed combustors, Chem. Eng. Sci. 45 (1990) 3123–3136.
[30] M.C. Lints, L.R. Glicksman, Parameters governing particle to wall heat transfer in a circulating fluidized bed, in: A.A. Avidan (Ed.), Circulating Fluidized Bed Technology IV, AIChE, New York, 1994, pp. 63–82.
[31] J. Werther, Fluid mechanics of large scale CFB units, in: A.A. Avidan (Ed.), Circulating Fluidized Bed Technology IV, AIChE J. (1994) 1–8.
[32] T.M. Knowlton, J.W. Carson, G.E. Klinzing, W.-C. Yang, Chem. Eng. Progr. (April) (1994) 44.
[33] Y.L. Ma, J.X. Zhu, Heat transfer in the downer and the riser of a circulating fluidized bed – a comparative study, Chem. Eng. Technol. 24 (2001) 85–90.
[34] Y. Hua, G. Flamant, J. Lu, D. Gauthier, 3D modeling of radiative heat transfer in circulating fluidized bed combustors: influence of the particulate composition, Int. J. Heat Mass Transfer 48 (2005) 1145–1154.
[35] M. Koksal, M.R. Golriz, F. Humdullahpur, Thermal aspects of a circulating fluidized bed with air staging, Int. J. Energy Res. 29 (2005) 923–935.
[36] F.P. Incropera, D.P. Witt, Fundamentals of Heat and Mass Transfer, John Wiley, New York, 2002.
[37] G. Flamant, Tranfert de chaleur couples dans les lits fluidises a haut temperature, Application a la conversion thermique de l'energie solaire, these de docteur Ea-Science 93, 1985.